NMR Structural Characterization of Peptide Inhibitors Bound to the Hepatitis C Virus NS3 Protease: Design of a New P2 Substituent

Nathalie Goudreau,*[,†] Dale R. Cameron,[†,‡] Pierre Bonneau,[§] Vida Gorys,[†] Céline Plouffe,[§] Martin Poirier,[†] Daniel Lamarre,[§] and Montse Llinas-Brunet[†]

Departments of Chemistry and Biological Sciences, Boehringer Ingelheim (Canada) Ltd., Research & Development, 2100 Cunard Street, Laval, Québec, Canada H7S 2G5

Received June 19, 2003

A comparative NMR conformational analysis of three distinct tetrapeptide inhibitors of the Hepatitis C NS3 protease that differ at the 4-aryloxy-substituted P2 proline position was undertaken. Specifically, transferred nuclear Overhauser effect experiments in combination with restrained systematic conformational searches were used to characterize the orientation of the P2 aryl substituents of these inhibitors when bound to the NS3 protease. Differences between free and bound conformations were also investigated. Analysis of the results allowed the design of a new P2 aromatic substituent, which significantly increased the potency of our inhibitors. The bound conformation of a specific competitive inhibitor having this novel P2 substituent is also described, along with a model of this inhibitor bound to the NS3 protease. This NS3 protease/inhibitor complex model also supports a hypothetical stabilization role for the P2 residue of the substrates and/or inhibitors and further elucidates the subtle details of the binding of the P2 residue of substrate-based inhibitors.

Introduction

Chronic Hepatitis C virus (HCV) infection is a major health problem that leads to cirrhosis, hepatocellular carcinoma, and liver failure in a substantial number of infected individuals, now estimated to be more than 170 million worldwide.[1] For many patients, the current therapies, which involve treatment with interferon α alone or in combination with the nucleoside analogue ribavirin, are not highly effective and result in severe side effects.[2] There is consequently an urgent need for the development of novel, specific, and more efficacious treatment strategies against this viral infection.

HCV is a small, enveloped virus containing a single positive strand RNA genome of approximately 9.6 kb. The genome carries a single long open-reading frame, which encodes a polyprotein of about 3000 amino acids. The HCV polyprotein, which is composed of structural proteins in its N-terminal portion and of nonstructural (NS) proteins in the remainder, is cleaved co- and posttranslationally by cellular and viral proteinases into at least 10 different products.[3]

The most intensively studied and best characterized target in the HCV genome is the NS3 serine protease, which is located within the N-terminal one-third (180 amino acids) of the NS3 protein.[4] This protease is responsible for the maturation of the viral polyprotein through cleavage at the NS3/4A, NS4A/B, NS4B/5A, and NS5A/B junctions. The first cleavage (NS3/4A) occurs rapidly and in cis, while the remaining three others occur in trans. Although the NS3 protease has proteolytic activity on its own in vitro, the presence of the NS4A protein, which acts as a cofactor, was shown to be essential for the cleavage of the NS4A/B and NS4B/5A junctions, whereas its presence enhances the cleavage efficiency at the NS5A/B junction.[5] The NS4A activator is a 54 residue polypeptide that forms a noncovalent complex with the NS3 protease. The crystal and the NMR solution structures of the uncomplexed NS3 protease domain have already been reported.[6,7] Both of these studies revealed that this enzyme adopts a canonical chymotrypsin-like fold consisting of N-terminal and C-terminal β-barrel domains, with the catalytic triad residues His57, Asp81, and Ser139 located in a deep cleft at the interface between these two domains. In addition, two X-ray structures of the NS3 protease in complex with a synthetic NS4A 12 residue cofactor peptide show that the NS4A peptide intercalates within the N-terminal β-sheet domain of the enzyme, resulting in a more ordered structure.[8,9] The combined structural data suggest that binding of the NS4A primarily affects the fold of the N-terminal domain of the NS3 protease, which corresponds to the S′ binding site of the substrates (as defined by Schechter and Berger nomenclature).[10]

The NS3 protease was shown to be essential for HCV replication and infection in the chimpanzee model, providing direct validation of this enzyme as a target for the development of new antiviral drugs.[11] In this respect, we and others have reported that N-terminal cleavage products of peptide substrates (S binding site) are competitive inhibitors of the NS3 protease activity.[12,13] This finding has served as the basis for designing substrate-based inhibitors, and our efforts in this area focused on improving the potency and on decreasing the peptidic character of these inhibitors. Starting with the hexapeptide Ac-DDIVPNva-OH as our original lead (IC_{50} = 150 μM), we found that a 400-fold increase in potency could be obtained by the introduction of a (4*R*)-

* To whom correspondence should be addressed. Tel: 450-682-4640. Fax: 450-682-4189. E-mail: ngoudreau@lav.boehringer-ingelheim.com.
† Department of Chemistry.
‡ Present address: Micrologix Biotech Inc., BC Research Complex, 3650 Wesbrook Mall, Vancouver, BC, V6S 2L2.
§ Department of Biological Sciences.

10.1021/jm0303002 CCC: $27.50
Published on Web 12/06/2003

Table 1. Tetrapeptide Inhibitors of the HCV NS3 Protease[14,21]

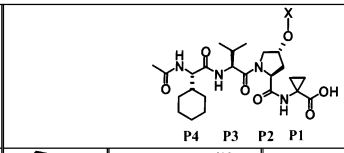

		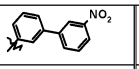		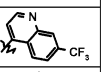
Compound #	**1**	**2**	**3**	**4**
IC_{50}	4 μM	4 μM	52 μM	8 μM

*IC_{50} values for these compounds were determined using a radiometric assay as previously described.[12]

naphthen-1-ylmethoxy substituent in the P2 proline (IC_{50} = 0.39 μM).[14] Further optimization was also obtained by replacing the P1 norvaline residue (Nva) of the original lead by the 1-amino-cyclopropylcarboxylic acid, resulting in a 3-fold increase in potency (IC_{50} = 54 μM).[14] In addition, by combining these two features, we were able to reduce the size of our inhibitors from hexa- to tetrapeptides with compound **1** having an IC_{50} in the low micromolar range (Table 1).[14] However, to further enhance the potency of these inhibitors, the knowledge of their structural features, either alone or in complex with the NS3 protease, became essential.

In recent years, a significant number of reports have appeared describing NMR and X-ray structural data of substrate-based peptidic inhibitors in interaction with the NS3 protease domain. First, we and others have reported the NS3 protease-bound conformations of C-terminal carboxylic acid hexapeptide inhibitors, as determined by transferred nuclear Overhauser effect (NOE) experiments.[15,16] These studies indicated that the bound inhibitors adopt a rather extended conformation. This finding was also reflected in the published crystal structure of the full length NS3 protease−helicase protein, in which the active site of the NS3 protease domain is occupied by the NS3 C terminus, thus providing an atomic view of the complex between the protease domain and the P side product of the cis cleavage reaction.[17] More recently, an NMR solution structure[18] and crystal structures[19] of complexes between the NS3 protease domain and the reversible covalently bound tripeptide α-ketoacid inhibitors provided a consistent view as to how these inhibitors bind to the NS3 protease, despite the fact that the NS4A cofactor peptide was present only in the X-ray crystal structures. A notable proposition from the NMR study[18] was that the P2 residue of the substrates and/or inhibitors may stabilize the catalytic His-Asp hydrogen bond by shielding the corresponding region of the protease from solvent.

Our own investigations have also explored the role of the P2 residues in our inhibitor series. As highlighted in our earlier structure−activity relationship (SAR) studies, a major gain in potency could be obtained by introducing different 4-arylmethyloxy-substituted prolines at the P2 position of our product-based inhibitors, with a 400-fold increase in potency attained by the introduction of a (4*R*)-naphthen-1-ylmethoxy substituent.[14] This significant finding prompted the NMR study of a tetrapeptide inhibitor (related to compound **1** in Table 1) with such a P2 substituent.[20] NMR line broadening experiments first demonstrated that the P2 naphthyl moiety was most probably located at the protein binding interface since the naphthyl resonances experience significant perturbations upon addition of the NS3 protease.[20] In addition, transferred NOE experiments showed that this tetrapeptide inhibitor adopted an extended bound conformation reminiscent of the previously studied hexapeptide analogue.[15] Unfortunately, in these earlier NMR studies, the determination of the precise bound orientation of the different P2 arylmethyloxy substituents was not possible, due to a lack of sufficient NOEs.[15,20]

To gain further insight into the binding mode of the P2 residues of our inhibitors, a comparative NMR conformational analysis of three tetrapeptide inhibitors, differing at the 4-aryloxy-substituted P2 proline position (compounds **2**−**4**; Table 1), was undertaken. These inhibitors are equipotent or slightly less potent than our reference compound **1**, which contains the 4-naphthylmethyloxy-substituted proline,[21] but as compared to **1**, they have one less rotatable bond at the level of P2 and thus can adopt a more restricted range of conformations. In addition, the nonsymmetric pattern of substitution in each of these P2 aromatic groups is of interest from an NMR viewpoint, since it eliminates the possibility of having magnetically equivalent protons. Finally, these three compounds highlight the diversity of aromatic substituents (phenyl, quinolyl, and biphenyl), which can be introduced at this position. In the work described below, transferred NOE experiments in combination with restrained systematic conformational searches were used to characterize the orientation of the P2 aryl substituents of compounds **2**−**4**, when bound to the NS3 protease. The differences between their free and bound conformations were also investigated. Analysis of these initial results allowed us to design a new P2 aromatic subtituent, which significantly increased potency when introduced on the proline of our standard tetrapeptide inhibitors. The bound conformation of a specific competitive inhibitor having this novel P2 substituent is also described, along with a model of this inhibitor bound to the NS3 protease.

Results and Discussion

Free vs Bound Conformations at P2. A transfer NOE experiment is a well-known NMR technique commonly used for determining the bound conformations of small molecules undergoing rapid exchange with a protein target.[22] In the first part of this study, this methodology was applied to analogues **2**−**4** in order to characterize the orientation of their P2 substituent when bound to the enzyme. In addition, the differences in the structural features of these inhibitors between their free and bound states were also monitored. This information may be useful for the design of conformationally restricted analogues that mimic the bound conformation.

Comparison of the NOE information between the free state (from ROESY spectra) and the bound state (from tr-NOESY data) showed that the P2 side chains of inhibitors **2** and **3** were significantly rigidified upon binding the NS3 protease. Indeed, while in the free state, the NMR data for these inhibitors suggested that their P2 side chains were flexible, and adopting multiple conformations (i.e., undergoing free rotation), the NOE

cross-peaks observed in the bound state were in contrast clearly indicating that their P2 aromatic substituents were getting locked in a well-defined conformation upon binding to the NS3 protease (see Supporting Information for more details).

In contrast to the similar conformational behavior of inhibitors **2** and **3**, the ROEs displayed for compound **4** in the free state suggested a less flexible P2 side chain that experienced less conformational averaging on the NMR time scale (i.e., less free rotation). In addition, the ensemble of NOEs observed for **4** in the free state was more similar to those observed in the bound state (Supporting Information). From an entropic viewpoint, this indicates that the quinolinyl derivative might represent a better P2 substituent because of its reduced flexibility, since properly constrained inhibitors are expected to bind their target more tightly (requiring a smaller decrease in the conformational entropy of binding than unconstrained or more flexible analogues).

The results obtained for these three inhibitors in the presence of the NS3 protease also provided information on the relative positions of their P2 and P4 side chains. Indeed, specific interresidue transferred NOEs were observed between the aromatic protons of their P2 substituents and the γ- and δ-protons of the P4 cyclohexyl glycine moiety, reflecting the proximity of these two side chains in the bound state (Supporting Information). This is consistent with one of our earlier reports in which the P2 and P4 side chains of an analogue of compound **1** were shown to lie close to one another in the bound state.[20] Interestingly, others have also reported this P2 and P4 proximity and suggested that the interactions between the hydrophobic side chains of these two positions could favor the bioactive conformation through hydrophobic collapse.[23] To test this hypothesis, these authors synthesized two tetrapeptide inhibitors in which the P2 and P4 side chains were connected via a biphenyl ether.[23] More recently, another group also reported a series of macrocyclic inhibitors comprising either N-cyclic or alkyl and aryl P2 moieties linked to the P4 residue via various ether linkages.[24] In sum, these data clearly highlight the P2 and P4 side chain proximity of substrate-based inhibitors in their NS3 protease bound states.

The tr-NOE data obtained for the above three inhibitors were subsequently used to determine their P2 bound conformations. Specifically, a systematic conformational search around the ether functionality linking the γ-carbon of the proline ring and the carbon atom of the aromatic groups was performed. This search included energy terms, as well as NOE restraints derived from the volume of the transferred NOE cross-peaks obtained in the presence of the NS3 protease. Figure 1 displays the superposition of the ensemble of low energy, transferred NOE consistent conformations for the P2 moiety of inhibitors **2**−**4**. The P2-bound conformations of analogue **2** were well-defined and characterized by having the second aromatic ring (ring B) of the biaryl moiety lying on the δ-side of the proline and pointing toward the P4 position. This is in full agreement with the observed P2−P4 interresidue NOEs. In contrast, a wider range of low energy, NMR consistent conformations was obtained for the P2 phenyl side chain of compound **3**. Despite this, the phenyl ring of **3** still

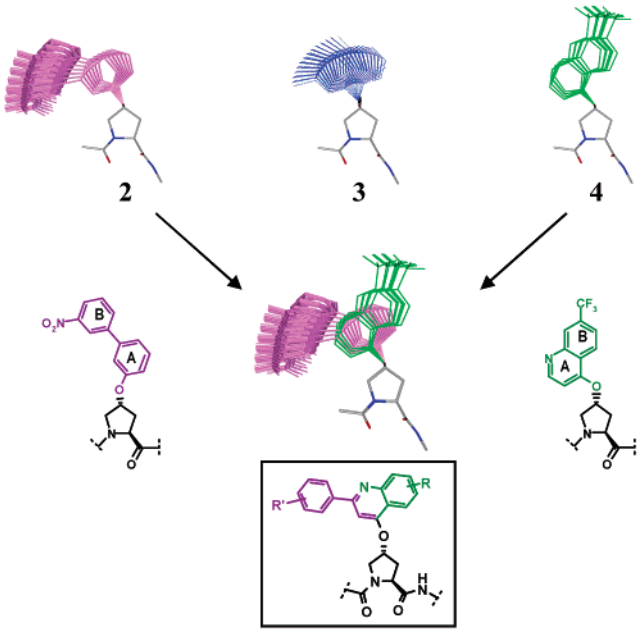

Figure 1. Superposition of the low-energy P2 side chain conformations of inhibitors **2**−**4** derived from a systematic conformational search that included NMR restraints derived from their NS3 protease bound states. Comparison of the P2 side chain bound conformations of analogues **2** and **4** and design of a new 2-aryl-substituted quinolyl P2 substituent.

adopts a bound conformation, which is very similar to the one adopted by the ring A of the biaryl moiety of **2** and which is characterized by the 3-bromine atom lying on the δ-side of the proline and pointing toward the P4 position (Figure 1). For inhibitor **4**, although the ring A of its P2 quinolyl moiety adopted a bound conformation that was very similar to those adopted by the phenyl rings of inhibitors **2** and **3**, the ring B portion of its quinolyl moiety was found to lie on the opposite β-side of the proline.

Design of an Improved P2 Substituent. Figure 1 also displays a superposition of the P2 bound conformations of analogues **2** and **4**. The A rings of these two inhibitors adopt very similar bound conformations, whereas their second aromatic rings (B ring) explore different regions of the conformational space and therefore occupy different binding areas. We hypothesized that a combination of the biaryl and quinolyl features into a single P2 substituent, through 2-phenyl-substituted quinolyl moieties as shown in Figure 1, should exploit the binding properties of both moieties.

As a starting point, the 2-phenyl-4-quinolinoxy derivative was synthesized[25] and introduced via a Mitsunobu reaction onto Boc-(4*S*)-cis-hydroxyproline methyl ester.[21] The 4-*R*-substituted proline ester was then hydrolyzed and sequentially coupled to the P1, P3, and P4 fragments, as described in the Experimental Section. In addition, this newly designed P2 substituent was introduced in two different series of inhibitors with distinct P1 residues.[26] The inhibitory activities of these new tetrapeptide inhibitors are reported in Table 2. Interestingly, compound **7**, which displays this novel P2 substituent, showed an approximated 10-fold increase in inhibitory activity ($IC_{50} = 0.37$ μM) when compared to the two reference compounds containing either the simple quinolyl or the biaryl substituents ($IC_{50} = 2$ and

Table 2. Novel Tetrapeptide Inhibitors of the HCV NS3 Protease Containing an Improved P2 Aromatic Substituent

X =				
	Compound #	**5**	**6**	**7**
	IC_{50}	2.2 μM	6.2 μM	0.37 μM
	Compound #	**8**	**9**	**10**
	IC_{50}	0.110 μM	0.120 μM	0.013 μM

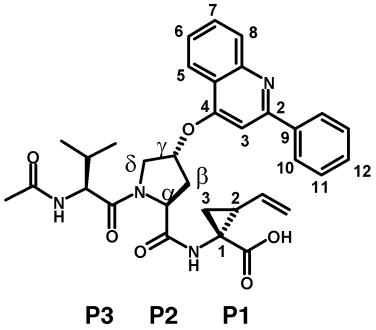

Figure 2. Chemical structure of the peptidic inhibitor **11**.

6 μM, respectively).[21] Moreover, when this new P2 substituent was introduced into a more optimized series containing the (1*R*)-amino, (2*S*)-vinyl cyclopropyl carboxylic acid derivative at P1,[26] a 9-fold increase in inhibitory activity was observed when compared to reference compounds **8** and **9**, giving rise to compound **10** that had low nanomolar potency (IC_{50} = 0.013 μM).

We wished to better understand the significant increase in the potency of inhibitors **7** and **10** by solving their NS3 protease-bound conformations. Unfortunately, these inhibitors were too potent for the use of transfer NOE type experiments, which require a fast on−off exchange rate of the inhibitor with the protein target. Although the bound conformation could be obtained from isotope labeling techniques and isotope-filtered NMR experiments,[27] we employed a simpler and less time-consuming approach. This consisted of truncating the P4 residues (Ac-Chg) in the above tetrapeptide inhibitors in order to render these inhibitors less potent and therefore amenable to transferred NOE experiments. This truncation approach was applied to inhibitor **10**, which belongs to our most optimized series of inhibitors.[26] Compound **11** (Figure 2) was therefore prepared using a synthetic scheme similar to the ones described previously.[21,26] As per design, this inhibitor displayed an IC_{50} of 3 μM, appropriate for transferred NOE type experiments.

NMR Study and Bound Conformation of a Newly Designed Peptidic Inhibitor. Figure 3A shows a region of the two-dimensional (2D) NOESY spectrum of inhibitor **11** recorded in the absence of the NS3 protease where only a few positive NOEs were observed, as expected for a small molecule of this size. In contrast, the NOESY recorded after the addition of the NS3 protease (22:1 inhibitor to protease ratio) showed an extensive set of new, negative-transferred NOE cross-peaks (Figure 3B). The observation of these transferred NOEs demonstrated the reversibility and the fast exchange binding of **11** to the NS3 protease. To confirm

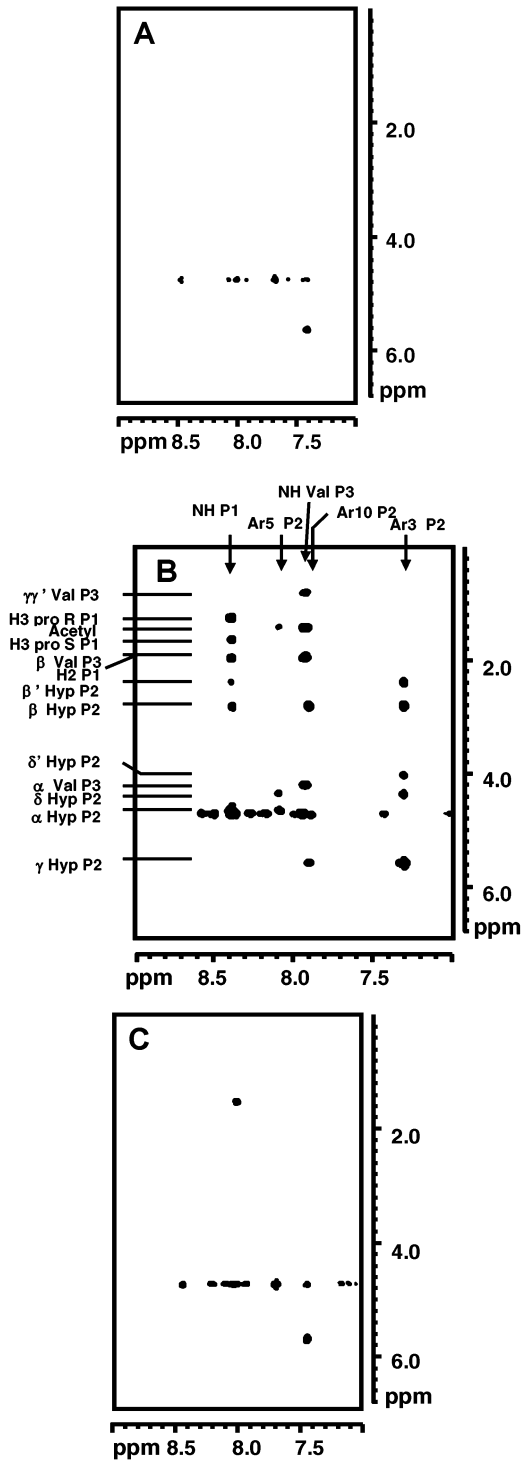

Figure 3. Amide/aromatic to aliphatic region of the 2D ^{1}H NMR spectra of inhibitor **11**. (A) NOESY spectrum (200 ms mixing time) of free **11**. (B) NOESY spectrum (200 ms mixing time) of **11** in the presence of NS3 protease BK poly Lys (22:1 inhibitor to protease ratio). (C) NOESY spectrum (200 ms mixing time) of **11** in the presence of NS3 protease and a potent competitive inhibitor (22:1:2.5 inhibitor to protease to potent inhibitor ratio). Resonance assignments for all three panels are summarized in B.

that these transferred NOEs originated from the binding of **11** to the enzyme active site, a competition experiment was performed. In this experiment, a potent hexapeptide inhibitor (IC_{50} = 23.5 nM)[28] containing a C-terminal α-ketoamide derivative, which is known to

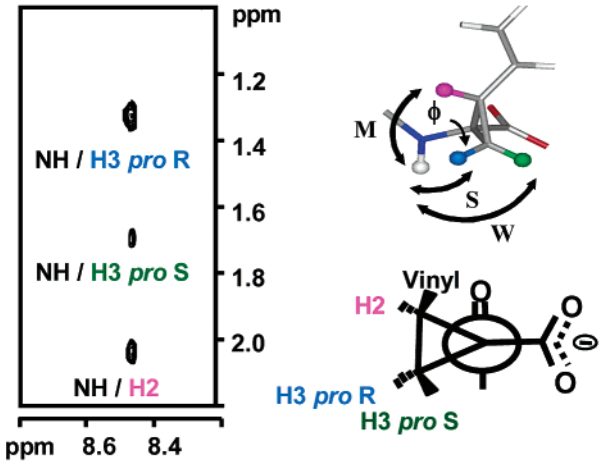

Figure 4. P1 amide to aliphatic region of the 2D ^{1}H NMR NOESY spectrum (200 ms mixing time) of **11** in the presence of NS3 protease BK poly Lys (22:1 inhibitor to protease ratio). The Newman projection representing the P1 ϕ angle as well as a molecular model highlighting the P1 bound conformation are also shown.

covalently and reversibly bind to the catalytic serine hydroxyl group and block the NS3 active site, was added to the inhibitor **11**/NS3 protease sample (at 2.5 times the concentration of the enzyme) and a NOESY spectrum was reacquired. As shown in Figure 3C, the previous set of transferred NOE cross-peaks disappeared and the spectrum of the free inhibitor was restored (Figure 3C vs A). This is a clear indication that inhibitor **11** was displaced from the NS3 active site by the serine trap-based inhibitor.

The bound conformational properties of inhibitor **11** were then studied in more detail. First, a set of transferred NOEs involving the aromatic protons of the 2-phenylquinoline substituent and the proline ring protons were observed in the presence of the NS3 protease (Figure 3B). Specifically, tr-NOEs between the aromatic protons 10 (refer to Figure 2 for atom numbering) and the β- and γ-protons of the proline ring and between the aromatic proton 5 and the δ-proline protons and the P3 acetyl group were observed (Figure 3B). The observation of these specific NOEs clearly indicated that the 2-phenyl substituent of the quinoline ring lies on the right-hand side of the inhibitor (toward the P1 portion) in the bound state. This was also corroborated by the absence of tr-NOEs between the aromatic protons 10 and the δ-proline protons and between the aromatic proton 5 and the β-proline protons. Tr-NOEs were also observed for the P1 residue of **11**. Of particular interest were those NOEs observed between the P1 NH and the cyclopropyl H3 *pro* R (strong), H2 (medium), and H3 *pro* S (weak) protons (Figure 4). As shown in this figure, the presence and the relative intensities of these specific NOEs are in many ways directly related to the bound ϕ angle value of the P1 residue.

The distance restraints derived from the volumes of all of the transferred NOE cross-peaks were then used in a simulated annealing protocol in order to generate an ensemble of bound conformations. Figure 5A displays a stereoview of the superposition of the 10 lowest energy, transferred NOE consistent structures of **11**. A well-defined, extended conformation is clearly evident with a root mean square deviation for the P1−P3 backbone atoms of 0.02 Å. Moreover, in these bound conformations, the P1 residue was characterized by a ϕ angle value of $\sim -90°$ (see also Figure 4). The side chain conformations were also well-defined, in particular those of the P1 and P2 residues. Specifically, the P2 hydroxyproline ring was characterized by a pseudoaxial conformation with its aromatic substituent adopting a perpendicular orientation relative to the proline ring plane, as shown in Figure 5B. This pseudoaxial conformation of the proline was previously observed for other inhibitors[15,20] and gives rise to a strong NOE between the β- and the δ-*pro* R protons of the proline ring (data not shown).

One interesting feature of the bound conformations of **11** was its P2 side chain orientation. Although the P2 side chain conformation of **11** was rather well-defined throughout our ensemble of NMR-derived bound structures, its orientation was opposite that expected based on the superposition of the P2 side chain-bound conformations of the quinoline and biaryl rings of analogue **2** and **4**, as illustrated in Figure 1. To further investigate this unexpected P2-bound side chain con-

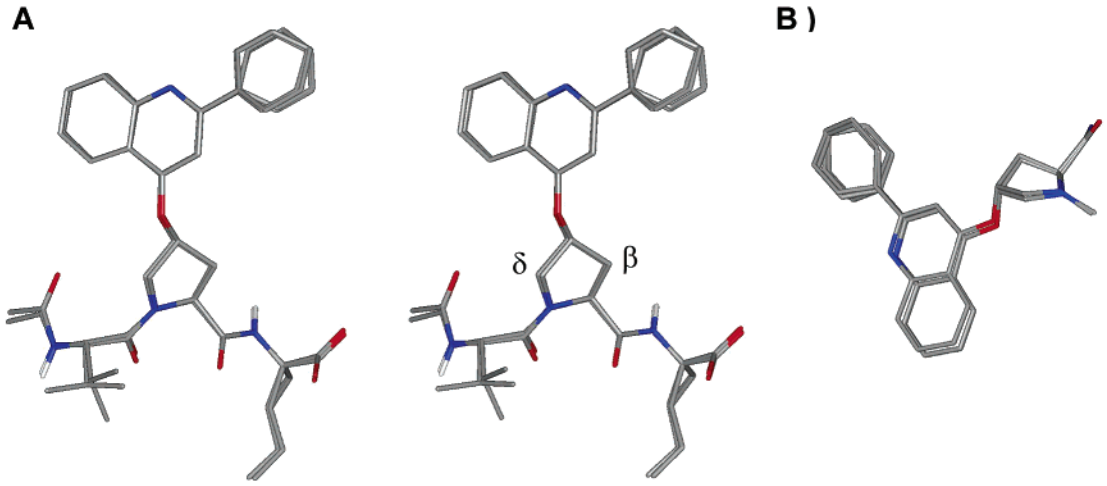

Figure 5. (A) Stereoview of the superposition (P1−P3 backbone atoms only) of the 10 best structures generated by restrained simulated annealing and derived from the NMR data of inhibitor **11** when bound to the NS3 protease. The structures are colored by atom type (oxygen is red, nitrogen is blue, carbon is dark gray, and hydrogen is light gray). Most of the hydrogen atoms are not shown. (B) Side view of the P2 residue conformations of the 10 best NMR-derived bound structures of **11**.

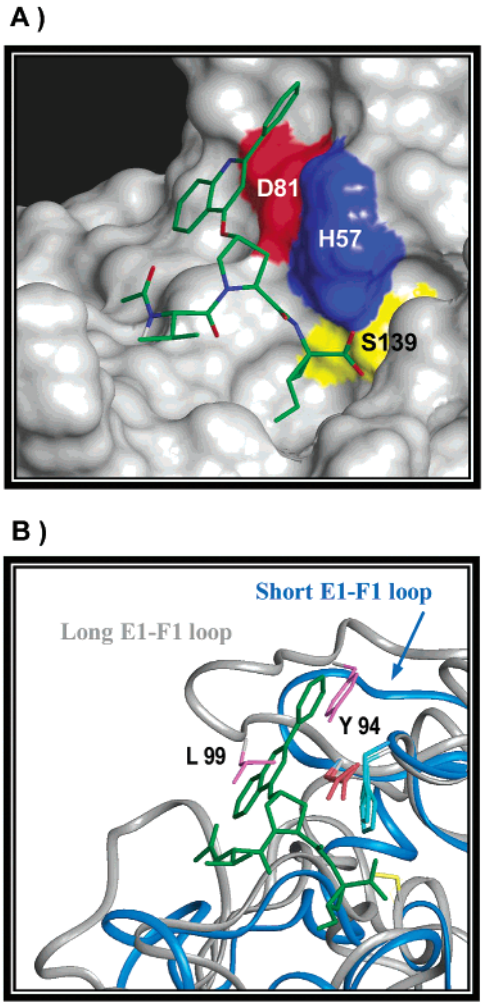

Figure 6. (A) Enlarged view of the active site of the NS3 protease/inhibitor **11** complex model. In this model, the NS3 protein is represented as a Conolly surface, while the inhibitor is represented in sticks and is colored by atom type. For clarity, most of the hydrogen atoms were omitted. (B) Ribbon representation of the superposition of the active site of NS3 protease/inhibitor **11** complex model onto the crystal structure of the HLE (PDB entry 1PPG).[33] The backbone and side chains of the three catalytic residues were used for the superposition (His57, Asp81, and Ser139 for NS3 protease vs His57, Asp102, and Ser195 for elastase).

formation, we generated a model of inhibitor **11** complexed to the NS3 protease.

Model of Inhibitor 11 Complexed with the NS3 Protease. The NMR-derived bound structure of inhibitor **11** was docked into the active site of the X-ray structure of the *apo* NS3 protease, using previously published crystal structures as a guide for the initial step of docking.[17,29−31] Specifically, the inhibitor was docked in such a way that it satisfied many of the hydrogen bonds that are observed in the crystal structure of the occupied active site of the full length NS3 protein.[17] This initial complex was energy-minimized and subsequently submitted to a 1 ns molecular dynamic simulation in a water droplet (see Experimental Section). The final model of this complex is shown in Figure 6A, in which inhibitor **11** extensively contacts the active site of the NS3 protease. Specifically, the backbone NH and CO groups of the P3 residues as well as the P1 NH are involved in an intermolecular, antiparallel β-sheetlike hydrogen bond network with the NS3 protease E2 strand (according to trypsin nomenclature).[6] In addition, the P1 acid group is stabilized via several hydrogen bonds involving the side chains of the active site residues His57 and Ser139 as well as the backbone amide protons of the oxyanion hole residues Gly137 and Ser139. This network of hydrogen bonds is in many ways reminiscent of those observed in the crystal structure of the full-length NS3 protein and/or the structures of other serine proteases complexed with peptides containing C-terminal carboxylic acids, which served as models for our initial docking step.[16,17,29−31] In addition, Figure 6A reveals that the P1 (1*R*)-amino, (2S)-vinyl cyclopropyl carboxylic acid derivative residue binds in the S1 pocket proximally positioned to the P3 valine side chain, a finding which we have recently exploited through the design and synthesis of potent P1−P3 macrocyclic inhibitors.[32]

Finally, in our model, the P2 proline ring packs against the side chain of Ala156 while its large aromatic substituent packs against the side chain of Arg155. In addition, the 2-phenyl substituent is positioned above the Asp81 carboxylate moiety, near the His57 imidazole moiety, and therefore partially shields these active site groups from solvent (Figure 6A).

Role of the P2 Substituent. Barbeto et al. proposed that the P2 residues of the substrates and/or inhibitors play a role in the stabilization of the catalytic His-Asp hydrogen bond, by shielding the corresponding region of the protease from solvent.[7,18] This hypothesis emerged from a comparison that was made using the structures of several members of the chymotrypsin-like family of serine proteases. This family of serine proteases has been divided into two subfamilies of structures: the short chain proteases (containing ~180 residues) and the long chain proteases (containing ~250 residues).[7] The long chain proteases are characterized by a nine residues long E1−F1 loop (Figure 6B) that shields the catalytic triad. In this specific subclass of serine proteases, the catalytic aspartate and histidine residues are shielded from the solvent by the side chains of two hydrophobic residues found on the E1−F1 loop at conserved positions (positions 94 and 99 in the case of many mammalian serine proteases such as trypsin, α-chymotrypsin, thrombine, and elastase).[7] For instance, in the crystallographic structure of the human leukocyte elastase (HLE), the conserved residues Tyr94 and Ile99 on the E1−F1 loop shelter the H-bond between the catalytic His57 and Asp102 (Figure 6B).[33] In addition, the presence of this long E1−F1 loop in these particular serine proteases somehow limits the space to accommodate the P2 position of the substrate, which typically consists of short chain amino acids (i.e., Gly or Ala).

In contrast, in short chain serine protease such as the NS3, the loop E1−F1 holding the catalytic Asp81 is only three residues long and therefore completely exposes the corresponding region to solvent (Figure 6B). Thus, the space to accommodate the P2 position of the substrate is significantly larger and explains the presence of bulkier side chains (such as those of Glu, Cys, Val, and Pro), which are the residues found in the natural substrates. Interestingly, Semliki Forest virus[34] and Sindbis virus[29,30] also encode similar short chain serine

proteases with a short E1−F1 loop and a solvent-exposed P2 region.

The results above as well as our previous SAR studies revealed a significant gain in inhibitor potency by introducing different hydrophobic substituents at the 4-position of their P2 proline, demonstrating that residues even bulkier than those found in the natural substrates can be accommodated and are beneficial at this position.[14,21] We have superimposed our model of inhibitor **11** complexed to the NS3 protease onto the crystal structure of the HLE,[33] as shown in Figure 6B. Quite interestingly, we can see from this figure that the 2-phenyl portion of the P2 substituent overlaps the position occupied by the conserved Tyr94 residue in the HLE structure, whereas the quinoline portion of the P2 substituent overlaps the position occupied by the HLE Leu99 residue. This observation suggests that our design has optimized a P2 substituent that mimics a natural stabilization role provided by two conserved hydrophobic residues at positions 94/99 in most long chain chymotrypsin-like serine proteases. Thus, one could predict that the best P2 substituents would be those that most optimally occupy both of these regions of the conformational space. Nonetheless, P2 substituents that only fill one of the two highlighted conformational spaces (such as those found in inhibitors **2**−**4**, for example) remain beneficial as shown in previous SAR studies,[14,21] although the factors that dictate the orientation of their P2 side chains in the bound state are not fully understood at this point and most probably involve other criteria such as hydrophobic and electronic properties.[21]

Our current results strongly support the hypothesis of Barbato et al. that the P2 residues of the NS3 protease substrate and/or inhibitor play a crucial role in stabilizing the catalytic machinery in the correct geometry by shielding that region of the protease from solvent.[18] In addition, through our current study, we have elucidated further critical details of the binding of the P2 residue of substrate-based inhibitors, which has ultimately led to the design of an improved P2 substituent.

Conclusions

In summary, the first part of this study has demonstrated that free vs bound conformation analysis can be useful for comparing and identifying optimal substituents from a series of related inhibitors. In addition, using NMR and computational chemistry data, we have successfully designed an improved P2 substituent for the proline residue of our current series of inhibitors. Using transferred NOE experiments and restrained simulated annealing, we have determined the NS3 protease-bound conformation of a smaller tripeptide inhibitor containing our novel 4*R*-(2-phenyl-quinolin-4-oxo) substituent on the P2 proline. Finally, an NS3 protease/inhibitor complex model was generated, which strongly supports the hypothetical stabilization role for the P2 residue of the substrates or inhibitors and which also further highlights the subtle details of the binding of the P2 residue of substrate-based inhibitors.

Experimental Section

Inhibitor Synthesis. The synthesis and characterization of compounds **1**−**6** were reported previously.[14,21] The synthesis of (1*R*,2*S*)-1-amino-2-vinyl-cyclopropyl carboxylic acid methyl ester used in the preparation of compounds **8**−**11** has been described [35] and will be reported elsewhere.[26]

Preparation of Boc-4-*R*-(biphenyl-3-yloxy)proline, Boc-4-*R*-(quinolin-4-yloxy)proline, and Boc-4-*R*-(2-phenyl-quinolin-4-yloxy)proline. The synthesis utilizes Boc-(4*S*)-*cis*-hydroxyproline methyl or benzyl ester and introduces the readily available 3-biphenyloxy, 4-quinolinoxy, or 2-phenyl-4-quinolinoxy[25] group via a Mitsunobu reaction using diethyl azodicarboxylate and triphenylphosphine reagents.[21] The 4-*R*-substituted proline ester was hydrolyzed using aqueous lithium hydroxide in tetrahydrofuran (THF).

Compounds 7−11. These inhibitors were prepared in solution by sequentially coupling either commercially available 1-aminocyclopropyl carboxylic acid methyl ester or (1*R*,2*S*)-1-amino-2-vinyl-cyclopropyl carboxylic acid methyl ester to the desired Boc-4-*R*-substituted proline using benzotriazol-1-yl-1,1,3,3-tetramethyluronium tetrafluoroborate (TBTU) as the coupling agent. Removal of the *N*-Boc protective group was effected with 4 N HCl in dioxane. The reaction sequence was applied again to the coupling of first Boc-valine and then Boc-cyclohexyl glycine. The acetyl capping group was introduced after removing the *N*-Boc protective group (as described above) and treating the N-terminal amine with acetic anhydride. Final hydrolysis of the methyl ester was done with aqueous LiOH in THF. The final compounds were purified by preparative high-performance liquid chromatography (HPLC) using either a Whatman Partisil 10-ODS-3 column, 2.2 cm × 50 cm, or a YMC Combi-Prep. ODS-AQ column, 50 mm × 20 mm ID, S-5 μm, 120 Å, and a linear gradient program from 2 to 100% acetonitrile/water (0.06% TFA). Fractions were analyzed by analytical HPLC, and the pure fractions were combined, concentrated, frozen, and lyophilized to yield the desired compound as the trifluoroacetate salt.

Inhibitor Characterization and Purity. NMR spectra were recorded on a Bruker AMX400 (400 MHz for ^{1}H NMR) spectrometer and were referenced to TMS as an internal standard (0 ppm δ scale). Data are reported as follows: chemical shift (ppm), multiplicity (s = singlet, d = doublet, t = triplet, br = broad, m = multiplet), coupling constant (J, reported to the nearest 0.5 Hz), and integration. High-resolution mass spectra were obtained from a Micomass AutoSpec instrument using fast atom bombardment (FAB) as the ionization mode with NBA as a matrix support. Inhibitor HPLC purity was measured by using an analytical C18 reversed phase column and two different eluting systems. Method A: 0.06% TFA in water−0.06% TFA in acetonitrile gradient (20−100% acetonitrile over 30 min); method B: 20 mM aqueous Na_2HPO_4 (pH 7.4)−acetonitrile gradient (20−75% acetonitrile over 25 min).

Compound 7. ^{1}H NMR (DMSO-d_6): ca, 1:7 mixture of rotamers; δ 8.76 and 8.44 (2xs, 1H), 8.28−8.19 (m, 3H), 8.19−8.11 (m, 1H), 7.98 (d, J = 8.0 Hz, 1H), 8.00−7.91 (m, 1H), 7.79−7.60 (m, 6H), 5.79 (bs, 1H), 4.51 (d, J = 11.9 Hz, 1H), 4.39 (dd, J = 8.6, J' = 17.0 Hz, 1H), 4.27 (dd, J = 8.4, J' = 16.8 Hz, 1H), 4.26−4.11 (m, 1H), 4.18 (dd, J = 7.8, J' = 16.0 Hz, 1H), 2.63−2.54 (m, 1H), 2.37−2.27 (m, 1H), 2.03−1.93 (m, 1H), 1.84 and 1.82 (2xs, 3H), 1.68−1.40 (m, 5H), 1.40−1.33 (m, 1H), 1.31−1.22 (m, 1H), 1.15−0.88 (m, 8H), 0.94 and 0.84 (2xd, J = 6.7 Hz, 3H), 0.89 and 0.78 (2xd, J = 6.9 Hz, 3H). HRMS: found, 698.3581; calcd for $C_{39}H_{48}N_5O_7$, 698.3554. HPLC: (a) 98.50%; (b) 99.43%.

Compound 8. ^{1}H NMR (DMSO-d_6): ca, 1:5 mixture of rotamers; δ 9.14 (d, J = 6.4 Hz, 1H), 8.64 and 8.60 (2xs, 1H), 8.32 (d, J = 8.3 Hz, 1H), 8.14−8.04 (m, 2H), 7.98 (d, J = 7.9 Hz, 1H), 7.82 (dd, J = 7.3, J' = 15.6 Hz, 1H), 7.66 (d, J = 8.6 Hz, 1H), 7.57 (d, J = 6.4 Hz, 1H), 5.77−5.63 (m, 2H), 5.21 (d, J = 8.6 Hz, 1H), 5.08 (d, J = 10.5 Hz, 1H), 4.50 (d, J = 12.1 Hz, 1H), 4.39 (dd, J = 8.6, 17.2 Hz, 1H), 4.22 (dd, J = 8.3, J' = 16.5 Hz, 1H), 4.24−4.05 (m, 2H), 2.60−2.50 (m, 1H), 2.38−2.26 (m, 1H), 2.05−1.95 (m, 1H), 1.84 and 1.82 (2xs, 3H), 1.70−1.38 (m, 8H), 1.28−1.22 (m, 1H), 1.10−0.85 (m, 5H), 0.94 (d, J = 6.7 Hz, 3H), 0.89 (d, J = 6.7 Hz, 3H). HRMS: found,

648.3401; calcd for $C_{35}H_{46}N_5O_7$, 648.3397. HPLC: (a) 98.76%; (b) 98.91%.

Compound 9. ^{1}H NMR (DMSO-d_6): ca, 1:6 mixture of rotamers; δ 8.78 and 8.58 (2xs, 1H), 7.90 (d, J = 8.6 Hz, 1H), 7.83 (d, J = 8.8 Hz, 1H), 7.69−7.60 (m, 1H), 7.66 (d, J = 7.2 Hz, 1H), 7.48−7.42 (m, 2H), 7.42−7.35 (m, 2H), 7.26 (d, J = 7.8 Hz, 1H), 7.16 and 7.13 (2xs, 1H), 6.94 (dd, J = 1.8, J' = 8.2 Hz, 1H), 5.77−5.64 (m, 1H), 5.22 (s, 1H), 5.19 (d, J = 6.7 Hz, 1H), 5.06 (d, J = 10.2 Hz, 1H), 4.37−4.25 (m, 2H), 4.25−4.16 (m, 1H), 4.07−3.94 (m, 2H), 2.34−2.26 (m, 1H), 2.16−2.09 (m, 1H), 2.07−1.97 (m, 1H), 1.84 and 1.83 (2xs, 3H), 1.68−1.46 (m, 7H), 1.26−1.20 (m, 1H), 1.18−0.78 (m, 6H), 0.90 (d, J = 6.7 Hz, 3H), 0.84 (d, J = 6.7 Hz, 3H). HRMS: found, 673.3588; calcd for $C_{38}H_{49}N_4O_7$, 673.3601; HPLC: (a) 96.53%; (b) 97.97%.

Compound 10. ^{1}H NMR (DMSO-d_6): ca, 1:5 mixture of rotamers; δ 8.82 and 8.58 (2xs, 1H), 8.31−8.24 (m, 2H), 8.20−8.14 (m, 1H), 8.13−8.04 (m, 1H), 7.98 (d, J = 8.0 Hz, 1H), 7.94−7.85 (m, 1H), 7.73 (s, 1H), 7.73−7.67 (m, 1H), 7.66−7.57 (m, 4H), 5.78−5.64 (m, 2H), 5.20 (dd, J = 1.6, J' = 17.5 Hz, 1H), 5.06 (dd, J = 1.3, J' = 10.5 Hz, 1H), 4.46 (d, J = 10.8 Hz, 1H), 4.39 (dd, J = 8.6, J' = 16.9 Hz, 1H), 4.29 (dd, J = 8.6, J' = 16.9 Hz, 1H), 4.23−4.15 (m, 1H), 4.08 (dd, J = 2.9, J' = 12.1 Hz, 1H), 2.34−2.24 (m, 1H), 2.06−1.97 (m, 2H), 1.85 and 1.82 (s, 3H), 1.70−1.42 (m, 7H), 1.28−1.22 (m, 1H), 1.05−0.87 (m, 6H), 0.95 and 0.85 (d, J = 6.7 Hz, 3H), 0.90 and 0.78 (d, J = 6.7 Hz, 3H). HRMS: found, 724.3710; calcd for $C_{41}H_{50}N_5O_7$, 724.3710. HPLC: (a) 96.45%; (b) 98.19%.

Compound 11. ^{1}H NMR (DMSO-d_6): ca, 1:6 mixture of rotamers; δ 8.76 and 8.58 (2xs, 1H), 8.28−8.21 (m, 2H), 8.18 (d, J = 8.3 Hz, 1H), 8.15−8.05 (m, 2H), 7.97−7.87 (m, 1H), 7.76−7.59 (m, 5H), 5.83−5.64 (m, 2H), 5.20 (d, J = 17.2 Hz, 1H), 5.07 (d, J = 10.2 Hz, 1H), 4.53−4.41 (m, 2H), 4.24 (dd, J = 8.3, J' = 16.9 Hz, 1H), 4.04 (d, J = 9.5 Hz, 1H), 2.68−2.59 (m, 1H), 2.38−2.26 (m, 1H), 2.08−1.93 (m, 2H), 1.57 (s, 3H), 1.61−1.46 (m, 2H), 1.28−1.22 (m, 1H), 0.91 (d, J = 6.4 Hz, 3H), 0.84 (d, J = 6.7 Hz, 3H). HRMS: found, 585.2712; calcd for $C_{33}H_{37}N_4O_6$, 585.2713. HPLC: (a) 97.86%; (b) 99.37%.

Biological Assays. The enzymatic assay was performed in 50 mM Tris-HCl, pH 8.0, 0.25 M sodium citrate, 0.01% (w/v) *n*-dodecyl-β-D-maltoside, 1 mM TCEP, 5 μM internally quenched fluorogenic peptide substrate anthranilyl-DDIVPAbu[C(O)-O]-AMY(3-NO_2)TW-OH, and various serially diluted concentrations of inhibitor were incubated with 1.5 nM NS3−NS4A heterodimer protein (genotype 1b) for 45 min at 23 °C. The final DMSO concentration did not exceed 5.25%. The reaction was terminated by the addition of 1 M MES, pH 5.8. Fluorescence of the N-terminal product was monitored on a BMG PolarStar Galaxy (excitation filter, 320 nm; emission filter, 405 nm). A nonlinear curve fit using the Hill model was then applied to the % inhibition concentration data, and the 50% effective concentration (IC_{50}) was calculated through the use of SAS (Statistical Software System, SAS Institute Inc., Cary, NC).

Expression and Purification of NS3 Protease. The NS3 protease domain was expressed in the pET29b vector (Novagen Inc.) and encoded a modified BK strain sequence that spanned amino acids 1−180. Work was also performed with this protease domain harboring a C-terminal poly Lys solubilization motif (ASKKKK).[13] The expression and purification protocol were as previously described[15] with the exception that a modified buffer (50 mM Na_2PO_4, 300 mM NaCl, 1 mM TCEP, pH 6.0) was used for the last Superdex 75 column. NMR stock solutions of the NS3 protease (~4.7 mg/mL for NS3 BK and ~9.2 mg/mL for NS3 BK poly Lys) were prepared by dialyzing the purified protein against a buffer containing either 50 mM deuterated sodium acetate, 350 mM NaCl, and 10 mM dithiothreitol-d_{10} (pH 6.5) for NS3 BK or 50 mM sodium phosphate, 300 mM NaCl, and 3 mM dithiothreitol-d_{10} (pH 6.5) for NS3 BK poly Lys, followed by concentration using a CentriCon-10 (Amicon).

NMR Sample Preparation. NMR samples were prepared by adding 24 μL of concentrated solution of inhibitors (either **2**, **3**, **4**, or **11**) in DMSO-d_6 to an aqueous buffer composed of either 50 mM CD_3CO_2Na, 350 mM NaCl, 10 mM dithiothreitol-d_{10}, and 10% (v/v) D_2O (spiked with 3-(trimethylsilyl)propionic 2,2,3,3-d_4 (TSP)) at pH 6.5 (for inhibitors **2**−**4**) or 50 mM Na_2PO_4, 300 mM NaCl, 3 mM dithiothreitol-d_{10}, and 10% (v/v) D_2O (spiked with TSP) at pH 6.5 (for inhibitor **11**). The final volume of these solutions was 600 μL with inhibitor concentrations ranging between 1 and 1.5 mM. To these samples was added a concentrated stock solution of NS3 protease (4.7 mg/mL, ~230 μM for NS3 BK and 9.2 mg/mL, ~ 450 μM for NS3 BK poly Lys) in a buffer identical to that described above such that an inhibitor/protease ratio of 20:1 to 50:1 was typically achieved. For the competition experiments, a stock solution of a potent activated carbonyl inhibitor (IC_{50} = 23.5 nM)[28] in DMSO-d_6 (3.6 mM) was added to the samples described above such that a 3−4-fold excess of potent inhibitor vs protease was achieved.

NMR Methods. All 2D spectra were acquired on a Bruker DRX 600 MHz NMR spectrometer equipped with a 5 mm TXI probe at 27 °C. Two-dimensional double quantum-filtered COSY (DQF-COSY), TOCSY, NOESY, and ROESY spectra were acquired using standard pulse sequences with the time proportional phase incrementation (TPPI) method. Suppression of the solvent signal was achieved by the use of presaturation or by inserting a 3-9-19 WATERGATE module prior to data acquisition.[36] The 2D transferred NOESY experiments were recorded with mixing times of 70, 100, 150, and 200 ms. In these experiments, a 25 ms spin-lock pulse was applied prior to t_1 delay in order to eliminate protein background signals.[37] The ROESY experiment was recorded with a 300 ms spin-lock period. The 2D data sets were typically acquired with 2048 points in t_2, 350−512 points in t_1, and 96−128 scans. The data were processed and analyzed using XWinNMR and WinNMR software (Bruker Canada, Milton, Ontario) and Felix software (Accelerys Inc., San Diego, CA). Shifted sine-bell apodization and zero-filling (2048 × 1048 real points) were applied prior to Fourier transformation, and subsequent baseline corrections were applied in one or both dimensions.

Restrained Systematic Conformational Search. This protocol was used in order to generate an ensemble of bound conformations for the P2 side chains of compounds **2**−**4** and combined systematic conformational search techniques with NMR-derived distance restraints. Specifically, a systematic conformational search by 5° increments around the two rotable bonds linking the γ-carbon of the proline ring to the carbon atom of the aromatic groups of **2**−**4** was performed using the Search Compare module of the InsightII software and the Discover 95.0 and the CFF97 force field (Accelerys Inc., San Diego, CA). In all of these searches, the proline ring was kept fixed. In addition to the energy terms, these searches also included distance restraints involving the P2 aromatic protons and the proline ring protons (β, γ, and δ), which were themselves derived from the volume of the transferred NOE cross-peaks obtained in the presence of the NS3 protease (Figures 1B and 3B for compounds **2** and **4**, respectively). These NMR distance restraints were applied as strong (1.8−2.5 Å), medium (1.8−3.5 Å), or weak (1.8−5.0 Å) flat-bottomed potentials with force constants of 30 kcal/mol Å^2. The conformations that were low in energy and NMR consistent for each inhibitor (compounds **2**−**4**) were selected at the end of this protocol and are shown superimposed in Figure 4.

Restrained Dynamics. The NS3-bound conformation of inhibitor **11** was modeled by a simulating annealing protocol using Discover 95.0 and the CFF97 force field (Accelerys Inc.). The dynamics were performed without cross-terms and nonbonded cutoffs and with a dielectric constant of 80. A total of 37 NMR-derived distance restraints were generated from transferred NOESY volume buildup rates using the Assign module of Felix software (Accelerys Inc.). These NMR distance restraints were applied as strong (1.8−2.5 Å), medium (1.8−3.5 Å), or weak (1.8−5.0 Å) flat-bottomed potentials with force constants of 30 kcal/mol·Å^2. Pseudoatoms defining the centroids of the methyl groups were introduced in the definition of the NOE restraints, and the interproton distances were corrected accordingly.[38] A single, high temperature unre-

strained dynamics run was performed at 900 K using a time step of 1 fs, with 50 structures collected at 2 ps intervals to generate a starting set of conformations. Each structure was then retrieved, cooled, and minimized using the following simulated annealing protocol. The temperature was initially lowered to 750 K at a rate of 30 K/ps where only strong restraints were applied. The remaining restraints were added and additional cooling to first 500 K (25 K/ps) and then 300 K (20 K/ps) was performed, followed by restrained minimization (including cross-terms) to a final gradient of 0.005 kcal/mol Å. A total of 10 low energy, NMR consistent structures were selected at the end of this protocol. These final 10 structures are shown superimposed (P1−P3 backbone atoms only). The root mean square deviation for the backbone atoms of P1−P3 is 0.02 Å. None of these structures have distance violations greater than 0.1 Å, and the average total restraint violation energy is 0.09 kcal/mol with a standard deviation = 0.03 kcal/mol.

Docking Protocol. The NS3 protease complex model of inhibitor **11** was obtained from energy minimization and molecular dynamics using Discover 95.0 and the CFF97 force field (Accelerys Inc.). The dynamics were performed without cross-terms and nonbonded cutoffs and with a dielectric constant of 1. As a starting point for the simulation, the NS3 protease-bound conformation of compound **11** (as determined above) was docked into the substrate binding region of the X-ray crystal structure of the *apo* NS3 protease.[9] The inhibitor was appropriately oriented in order to allow its P1 carboxylate group to make H-bonds with the side chains of the catalytic triad residues His57 and Ser139, as well as with the backbone NH of the oxyanion hole residues Ser139 and Gly137 and in order to allow the formation of additional hydrogen bonds between the backbone NH and CO groups of the inhibitor P3 and the complementary backbone groups of the protein Ala157 residue. The bound inhibitor was then energy-minimized. The conformations of the protein and of the inhibitor P1 carboxylate were kept fixed during this first minimization step. This initial complex model was subsequently soaked in a 20 Å sphere of water. The NS3 protein and the water molecules were then divided into three zones and tethered to different extents during the simulation: zone 1, 0−10 Å away from the center of mass of the inhibitor; zone 2, 10−15 Å away from the inhibitor; zone 3, >15 Å away from the inhibitor. The entire complex was first submitted to energy minimization and then to 1 ns of dynamics at 298 K following a 200 ps equilibration step. Zone 3 was kept fixed during this entire simulation, while zones 2 and 1 were tethered using quadratic force constants of 10 and 1 kcal/mol Å^2, respectively, during the initial minimization step. These tethering force constants were then gradually reduced during the dynamic equilibration steps and were totally removed during the 1 ns dynamic run. In addition, the inhibitor P1 carboxylate was also tethered using a quadratic force constant of 1 kcal/mol Å^2 during the initial steps. The bond lengths and water molecule angles were kept fixed during the entire dynamic simulation using a rattle. At the end of the dynamics, the complex was further minimized (including cross-terms) to a final gradient of 0.1 kcal/mol Å.

Acknowledgment. We thank Dr. Youla Tsantrizos for providing compounds **2**−**5**. We also thank Diane Thibeault and Roger Maurice for IC_{50} determination and Dr. George Kukolj for the preparation of the NS3 protease construct. Norman Aubry, Colette Boucher, and Serge Valois are acknowledged for excellent analytical support. We are also grateful to Dr. Steven LaPlante for helpful discussions and Drs. George Kukolj and Peter White for critical reading of the manuscript. Finally, we thank Drs. Paul Anderson, Michael Bös, Michael Cordingley, and Robert Déziel for encouragement and support.

Supporting Information Available: NMR data describing the free vs bound conformational analysis of the P2 substituent of inhibitors **2** and **4** as well as the NMR data showing the interresidue transferred NOEs between the P2 and the P4 side chains of inhibitor **2**. This material is available free of charge via the Internet at http://pubs.acs.org.

References

(1) Dymock, B. W.; Jones, P. S.; Wilson, F. X. Novel approaches to the treatment of Hepatitis C virus infection. *Antiviral Chem. Chemother.* **2000**, *11*, 79−96 and reference therein.

(2) McHutchison, J. G.; Gordon, S. C.; Schiff, E. R.; Shiffman, M. L.; Lee, W. M.; Rustgi, V. K.; Goodman, Z. D.; Ling, M.-H.; Cort, S.; Albrecht, J. K. Interferon-alpha-2b alone or in combination with ribavirin as initial treatment for chronic hepatitis C. *N. Engl. J. Med.* **1998**, *339*, 1485−1492.

(3) Bartenschlager, R.; Lohmann, V. Replication of hepatitis C virus. *J. Gen. Virol.* **2000**, *81*, 1631−1648.

(4) (a) Shoemaker, K. R. Recent progress on NS3 protease as an HCV drug target. *Curr. Opin. Anti-infective Invest. Drugs* **1999**, *5*, 559−564. (b) De Franscesco, R.; Steinkühler, C. Structure and function of hepatitis C virus NS3−NS4A serine proteinase. *Hepatitis C Viruses* **2000**, *242*, 149−169. (c) Steinkühler, C.; Koch, U.; Narjes, F.; Matassa, V. G. Hepatitis C virus serine protease inhibitors: current progress and future challenges. *Curr. Med. Chem.* **2001**, *8*, 919−932. (d) Walker, M. P.; Yao, N.; Hong, Z. Promising candidates for the treatment of chronic hepatitis C. *Exp. Opin. Invest. Drugs* **2003**, *12* (8), 1269−1280.

(5) Bartenschlager, R. The NS3/4A proteinase of the hepatitis C virus: unravelling structure and function of an unusual enzyme and prime target for antiviral therapy. *J. Viral Hepatitis* **1999**, *6*, 165−181 and references therein.

(6) Love, R. A.; Parge, H. E.; Wickersham, J. A.; Hostomsky, Z.; Habuka, N.; Moomaw, E. W.; Adachi, T.; Hostomska, Z. The crystal structure of hepatitis C virus NS3 proteinase reveals a trypsin-like fold and a structural zinc binding site. *Cell* **1996**, *87*, 331−342.

(7) Barbato, G.; Cicero, D. O.; Nardi, M. C.; Steinkühler, C.; Cortese, R.; De Franscesco, R.; Bazzo, R. The solution structure of the N-terminal proteinase domain of the hepatitis C virus (HCV) NS3 protein provides new insights into its activation and catalytic mechanism. *J. Mol. Biol.* **1999**, *289*, 371−384.

(8) Kim, J. L.; Morgenstern, K. A.; Lin, C.; Fox, T.; Dwyer, M. D.; Landro, J. A.; Chambers, S. P.; Markland, W.; Lepre, C. A.; O'Malley, E. T.; Harbeson, S. L.; Rice, C. M.; Murcko, M. A.; Caron, P. R.; Thomson, J. A. Crystal structure of the hepatitis C virus NS3 protease domain complexed with a synthetic NS4A cofactor peptide. *Cell* **1996**, *87*, 343−355.

(9) Yan, Y.; Li, Y.; Munshi, S.; Sardana, V.; Cole, J. L.; Sardana, M.; Steinkuehler, C.; Tomei, L.; De Franscesco, R.; Kuo, L. C.; Chen, Z. Complex of the NS3 protease and NS4A peptide of BK strain hepatitis C virus: A 2.2 Å resolution structure in a hexagonal crystal form. *Protein Sci.* **1998**, *7*, 837−847.

(10) Schechter, I.; Berger, A. On the size of the active site in proteases. I. Papain. *Biochem. Biophys. Res. Commun.* **1967**, *27*, 157−162.

(11) Kolykalov, A.; Mihalik, K.; Feinstone, S. M.; Rice, C. M. Hepatitis C virus-encoded enzymatic activities and conserved RNA elements in the 3′ nontranslated region are essential for virus replication in vivo. *J. Virol.* **2000**, *74*, 2046−2051.

(12) Llinàs-Brunet, M.; Bailey, M.; Fazal, G.; Goulet, S.; Halmos, T.; LaPlante, S.; Maurice, R.; Poirier, M.; Poupart, M.-A.; Thibeault, D.; Wernic, D.; Lamarre, D. Peptide-based inhibitors of the hepatitis C virus serine protease. *Bioorg. Med. Chem. Lett.* **1998**, *8*, 1713−1718.

(13) Steinkühler, C.; Biasiol, G.; Brunetti, M.; Urbani, A.; Koch, U.; Cortese, R.; Pessi, A.; De Francesco, R. Product inhibition of the hepatitis C virus NS3. *Biochemistry* **1998**, *37*, 8899−8905.

(14) Llinàs-Brunet, M.; Bailey, M.; Fazal, G.; Ghiro, E.; Gorys, V.; Goulet, S.; Halmos, T.; Maurice, R.; Poirier, M.; Poupart, M.-A.; Rancourt, J.; Thibeault, D.; Wernic, D.; Lamarre, D. Highly potent selective peptide-based inhibitors of the hepatitis C virus serine protease. Towards smaller inhibitors. *Bioorg. Med. Chem. Lett.* **2000**, *10*, 2267−2270.

(15) LaPlante, S. R.; Cameron, D. R.; Aubry, N.; Lefebvre, S.; Kukolj, G.; Maurice, R.; Thibeault, D.; Lamarre, D.; Llinàs-Brunet, M. Solution structure of substrate-based ligands when bound to Hepatitis C virus NS3 protease-domain. *J. Biol. Chem.* **1999**, *26*, 18618−18624.

(16) Cicero, D. O.; Barbato, G.; Koch, U.; Ingallinella, P.; Bianchi, E.; Nardi, M. C.; Steinkühler, C.; Cortese, R.; Matassa, V. G.; De Franscesco, R.; Pessi, A.; Bazzo, R. Structural characterization of the interactions of optimized product inhibitors with the N-terminal proteinase domain of the hepatitis C virus (HCV) NS3 protein by NMR and modeling studies. *J. Mol. Biol.* **1999**, *289*, 385−396.

(17) Yao, N.; Reichet, P.; Taremi, S. S.; Prosise, W. W.; Weber, P. C. Molecular views of viral polyprotein processing revealed by the crystal structure of the hepatitis C virus bifunctional protease-helicase. *Structure* **1999**, *11*, 1353−1363.
(18) Barbato, G.; Cicero, D. O.; Cordier, F.; Narjes, F.; Gerlach, B.; Sambucini, S.; Grzesiek, S.; Matassa, V. G.; De Franscesco, R.; Bazzo, R. Inhibitor binding induces active site stabilization of the HCV NS3 protein serine protease domain. *EMBO J.* **2000**, *6*, 1195−1206.
(19) Di Marco, S.; Rizzi, M.; Volpari, C.; Walsh, M. A.; Narjes, F.; Colarusso, S.; De Franscesco, R.; Matassa, V. G.; Sollazzo, M. Inhibition of the hepatitis C virus NS3/4A protease: the crystal structures of two protease-inhibitor complexes. *J. Biol. Chem.* **2000**, *275*, 7152−7157.
(20) LaPlante, S. R.; Aubry, N.; Bonneau, P. R.; Kukolj, G.; Lamarre, D.; Lefebvre, S.; Li, H.; Llinàs-Brunet, M.; Plouffe, C.; Cameron, D. R. NMR line-broadening and transferred NOESY as a medicinal chemistry tool for studying inhibitors of the Hepatitis C virus NS3 protease domain. *Bioorg. Med. Chem. Lett.* **2000**, *10*, 2271−2274.
(21) Poupart, M.-A.; Cameron, D. R.; Chabot, C.; Ghiro, E.; Goudreau, N.; Goulet, S.; Poirier, M.; Tsantrizos, Y. S. Solid-phase synthesis of peptidomimetic inhibitors for the Hepatitis C virus NS3 protease. *J. Org. Chem.* **2001**, *66*, 4743−4751.
(22) Ni, F. Recent developments in transferred NOE methods. *Prog. Nucl. Magn. Reson. Spectrosc.* **1994**, *26*, 517−606.
(23) Marchetti, A.; Ontaria, J. M.; Matassa, V. G. Synthesis of two novel cyclic biphenyl ether analogues of an inhibitor of HCV NS3 protease. *Synlett* **1999**, *S1*, 1000−1002.
(24) (a) Schering Corporation; Chen, K. X.; Arasappan, A.; Venkatraman, S.; Parekh, T. N.; Gu, H.; Njoroge, F. G.; Girijavallabhan, V. M.; Ganguly, A.; Sakena, A.; Jao, E.; Yao, N. H.; Prongay, A. J.; Madison, V. S.; Vibulbhan, B. Macrocyclic NS3-serine protease inhibitors of Hepatitis C virus comprising N-cyclic P2 moieties; WO-0177113, 2001. (b) Schering Corporation; Venkatraman, S.; Chen, K. X.; Arasappan, A.; Njoroge, F. G.; Girijavallabhan, V. M.; han, T. Y.; Mckittrick, B. A.; Prongay, A. J.; Madison, V. S. Macrocyclic NS3-serine protease inhibitors of Hepatitis C virus comprising alkyl and aryl alanine P2 moieties; WO-0181325, 2001.
(25) Giardina, G. A. M.; Sarau, H. M.; Farina, C.; Medhurst, A. D.; Grugni, M.; Raveglia, L. F.; Schmidt, D. B.; Rigolio, R.; Luttmann, M.; Vecchietti, V.; Hay, D. W. P. Discovery of novel class of selective non-peptide antagonists for the human neurokinin-3 receptor. *J. Med. Chem.* **1997**, *40*, 1794−1807.
(26) Rancourt, J.; et al. Manuscript in preparation.
(27) James, T. L.; Oppenheimer, N. J. Methods in Enzymology. *Nuclear Magnetic Resonance Part C*; Academic Press: San Diego, CA, 1994.
(28) Llinàs-Brunet, M.; Bailey, M.; Deziel, R.; Fazal, G.; Gorys, V.; Goulet, S.; Halmos, T.; Maurice, R.; Poirier, M.; Poupart, M.-A.; Rancourt, J.; Thibeault, D.; Wernic, D.; Lamarre, D. Studies on the C-terminal of hexapeptide inhibitors of the hepatitis C virus serine protease. *Bioorg. Med. Chem. Lett.* **1998**, *8*, 2719−2724.
(29) Choi, H. K.; Tong, L.; Minor, W.; Dumas, P.; Boege, U.; Rossmann, M. G.; Wengler, G. Structure of Sindbis virus core protein reveals a chymotrypsin-like proteinase and the organization of the virion. *Nature* **1991**, *345*, 37−43.
(30) Tong, L.; Wengler, G.; Rossmann, M. G. Refined structure of Sindbis virus core protein and comparison with other chymotrypsin-like serine proteinanses structures. *J. Mol. Biol.* **1993**, *230*, 228−247.
(31) James, M. N. G.; Sielecki, A. R.; Brayer, G. D.; Delbaere, L. T. J. Structures of product and inhibitor complexes of *Streptomyces griseus* protease at 1.8 Å resolution. A model for serine protease catalysis. *J. Mol. Biol.* **1980**, *144*, 43−88.
(32) Tsantrizos, Y. S.; Bolger, G.; Bonneau, P.; Cameron, D. R.; Goudreau, N.; Kukolj, G.; LaPlante, S. R.; Llinas-Brunet, M.; Nar, H.; Lamarre, D. Macrocyclic inhibitors of the NS3 protease as potential therapeutic agents of Hepatitis C virus infection. *Angew. Chem.* **2003**, *42*, 1355−1360.
(33) Wei, Z.; Mayr, I.; Bode, W. The refined 2.3 Å crystal structure of human leukocyte elastase in a complex with a valine chloromethyl ketone inhibitor. *Febs Lett.* **1988**, *234*, 367−372.
(34) Choi, H. K.; Lu, G.; Lee, S.; Wengler, G.; Rossmann, M. G. Structure of Semliki forest virus core protein. *Proteins: Struct. Funct. Genet.* **1997**, *27*, 345−359.
(35) Llinas-Brunet, M.; Bailey, M. D.; Cameron, D. R.; Faucher, A. M.; Ghiro, E.; Goudreau, N.; Halmos, T.; Poupart, M. A.; Rancourt, J.; Tsantrizos, Y. S.; Simoneau, B. Hepatitis C inhibitor tri-peptides; WO 00/09543, 2000.
(36) Sklenar, V.; Piotto, M.; Leppik, R.; Saudek, V. Gradient-tailored water suppression for ^{1}H-^{15}N HSQC experiments optimized to retain full sensitivity. *J. Magn. Reson. A* **1993**, *102*, 241−245.
(37) Scherf, T.; Anglister, J. A $T_{1\rho}$-filtered two-dimensional transferred NOE spectrum for studying antibody interactions with peptide antigens. *Biophys. J.* **1993**, *64*, 754−761.
(38) Wüthrich, K.; Billeter, M.; Braun, W.; Anglister, J. Pseudostructures for the 20 common amino acids for use in studies of protein conformations by measurements of intramolecular proton−proton distance constraints with nuclear magnetic resonance-filtered two-dimensional transferred NOE spectrum for studying antibody interactions with peptide antigens. *J. Biol. Mol.* **1983**, *169*, 949−961.

JM0303002